

Supporting Information for:

New insight into the material parameter B to understand the enhanced thermoelectric performance of $\text{Mg}_2\text{Sn}_{1-x-y}\text{Ge}_x\text{Sb}_y$

Weishu Liu¹, Jiawei Zhou², Qing Jie¹, Yang Li³, Hee Seok Kim¹, Jiming Bao³, Gang Chen^{2*}, and Zhifeng Ren^{1*}

¹Department of Physics and TcSUH, University of Houston, Houston, Texas 77204, USA

²Department of Mechanical Engineering, Massachusetts Institute of Technology, Cambridge, Massachusetts 02139, USA

³Department of Electrical and Computer Engineering, University of Houston, Houston, Texas 77204, USA

* To whom correspondence should be addressed: gchen2@mit.edu, zren@uh.edu

Table S1 Physical property of selected thermoelectric materials.

Short name	Composition	$(ZT)_{\max}$	m^*	U^*	κ_{lat}	E_g	B^*	Ref.
		[/]	[m_0]	[$\text{m K}^{-3/2} \text{s}^{-1} \text{V}^{-1}$]	[$\text{W m}^{-1} \text{K}^{-1}$]	[eV]	[/]	
Mg_2Sn	$\text{Mg}_2\text{Sn}_{0.99}\text{Sb}_{0.01}$	0.65, 350 °C	2.04	130.28	2.55	0.250	0.85	c)
$\text{Mg}_2\text{Sn}_{0.75}\text{Ge}_{0.25}$	$\text{Mg}_2\text{Sn}_{0.73}\text{Ge}_{0.25}\text{Sb}_{0.02}$	1.4, 450 °C	3.5	162.84	1.26	0.318	2.73	c)
CoSbTe	$\text{CoSb}_{2.85}\text{Te}_{0.15}$	0.9, 550 °C	-	^{a)} 98.73	1.94	^{b)} 0.275	0.93	43
CoSbTeSn	$\text{CoSb}_{2.75}\text{Te}_{0.20}\text{Sn}_{0.05}$	1.1, 550 °C	-	^{a)} 88.33	1.05	^{b)} 0.274	1.54	47
Ingot-BiSbTe	n.a.	1.4, 50 °C	-	^{a)} 207.13	0.88	^{b)} 0.168	2.64	48
Nano-BiSbTe	n.a.	1.05, 100 °C	-	^{a)} 194.06	0.52	^{b)} 0.184	4.58	48
Nano-BiTeSe	as-pressed $\text{Cu}_{0.01}\text{Bi}_2\text{Te}_{2.7}\text{Se}_{0.3}$	0.9, 100 °C	0.97	121.62	0.68	^{b)} 0.11	1.31	49
PbTe-1	$\text{Tl}_{0.02}\text{Pb}_{0.98}\text{TeSi}_{0.02}\text{Na}_{0.02}$	1.7, 500 °C	-	^{a)} 60.15	0.50	^{b)} 0.44	3.53	50
PbTe-2	PbTe: 6% MgTe	2, 550 °C	7	56.00	0.54	^{b)} 0.6	4.15	51
FeNbSb	$\text{FeNb}_{0.8}\text{Ti}_{0.2}\text{Sb}$	1.1, 827 °C	1.2	144.35	2.5	0.54	2.08	52

Note: a) estimated from measured σ and S according to the Ref. [*Chem. Mater.* 2008, **20**, 7526-7531.], and hence no carrier effective mass m^* available; b) estimated from $E_g = 2eS_{\max}T$; c) this study.

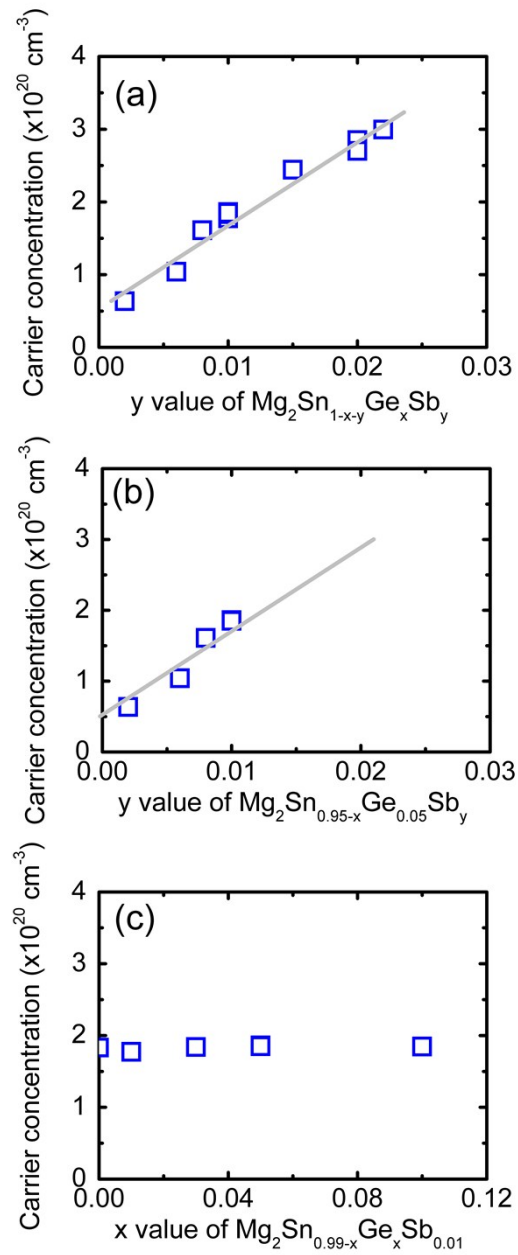


Fig. 1S. Carrier concentration as a function of Sb content and Ge content for sample $\text{Mg}_2\text{Sn}_{1-x-y}\text{Ge}_x\text{Sb}_y$. It is clearly shown that the carrier concentration varies with Sb rather than Ge in $\text{Mg}_2\text{Sn}_{1-x-y}\text{Ge}_x\text{Sb}_y$.

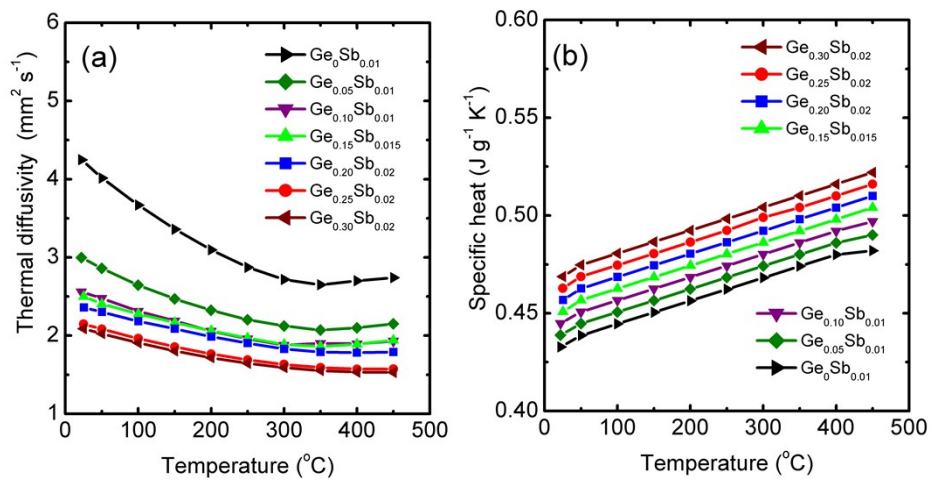


Fig. 2S. Temperature dependent diffusivity and specific heat of $\text{Mg}_2\text{Sn}_{1-x-y}\text{Ge}_x\text{Sb}_y$. (a) Thermal diffusivity, (b) specific heat.

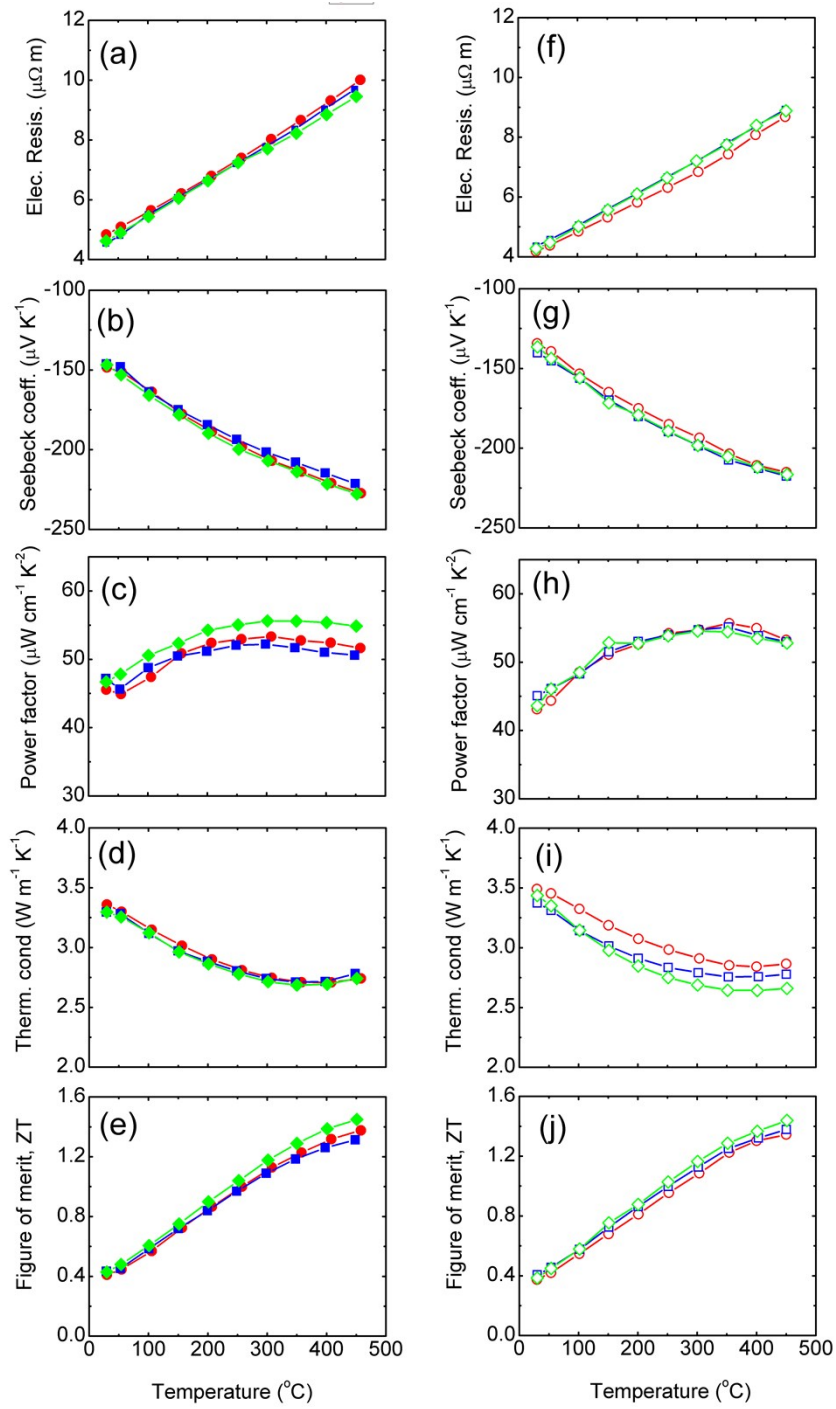


Fig. S3. Reproducibility of thermoelectric properties of $\text{Mg}_2\text{Sn}_{0.75-y}\text{Ge}_{0.25}\text{Sb}_y$. (a-e) Samples of $\text{Mg}_2\text{Sn}_{0.73}\text{Ge}_{0.25}\text{Sb}_{0.02}$ with carrier concentration of $2.7 \times 10^{20} \text{ cm}^{-3}$, and (f-j) samples of $\text{Mg}_2\text{Sn}_{0.728}\text{Ge}_{0.25}\text{Sb}_{0.022}$ with carrier concentration of $3.0 \times 10^{20} \text{ cm}^{-3}$.

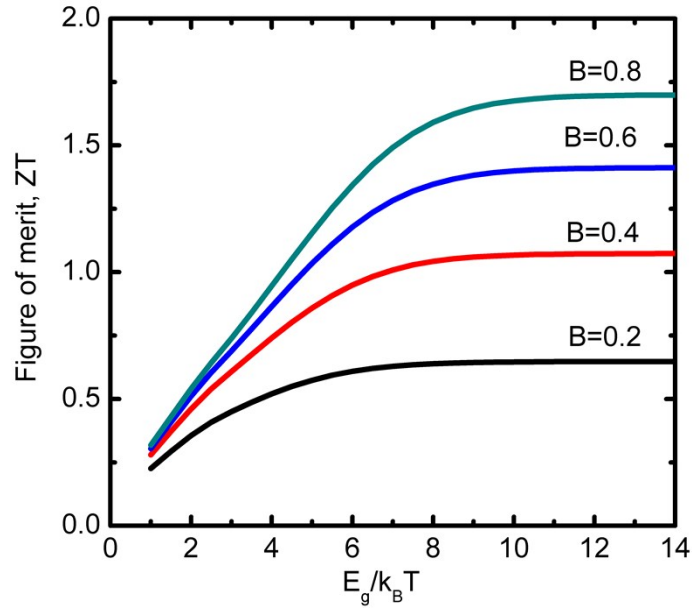


Fig. S4. Optimized ZT regarding with Fermi energy as a function of reduced band gap for the traditional material parameter $B = 0.2$ (bottom curve), 0.4, 0.6, and 0.8 (top curve) for the assumption of $s = -1/2$, $\xi_f = 0$, $U_e = U_h$ and $T = 300\text{K}$. This shows the effect of band gap using the traditional material parameter B and is consistent with Mahan's previous work [*J. Appl. Phys.*, 1989, **65**, 1578-1583.]

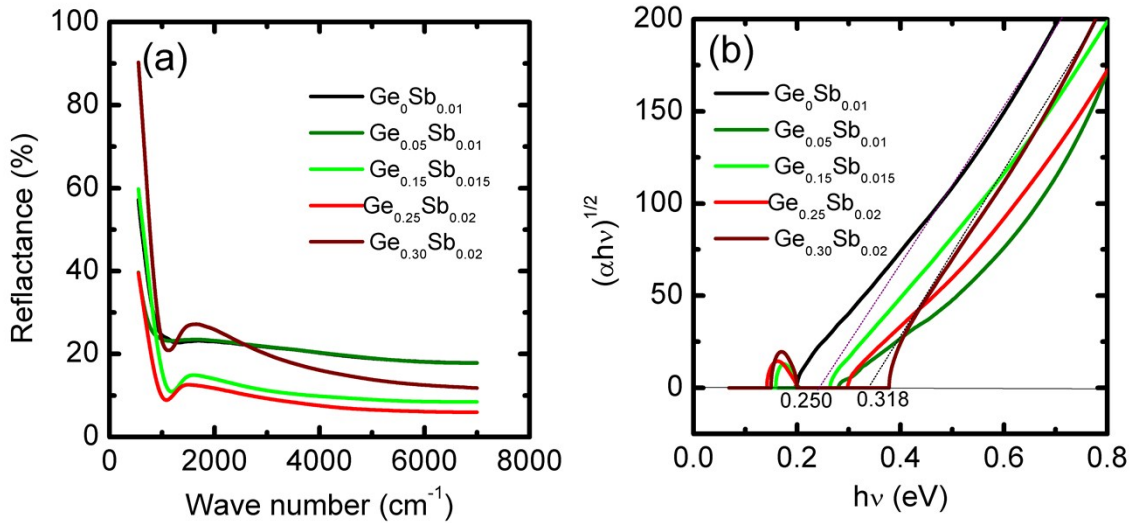


Fig. S5. (a) Reflectance spectrum of $\text{Mg}_2\text{Sn}_{1-x-y}\text{Ge}_x\text{Sb}_y$, (b) absorption spectra of $\text{Mg}_2\text{Sn}_{1-x-y}\text{Ge}_x\text{Sb}_y$ where the across point of the dash line with $h\nu$ axis was used to determine the band gap.

A. Expression of ZT by using Fermi–Dirac statistics in a two-band model

We consider two simple band, i.e. one parabolic conduction band and one parabolic valence band. By applying Simon's theory [J. Appl. Phys. 33, 1830 (1962)] the electrical conductivity σ , Seebeck coefficient S , and thermal conductivity κ could be expressed by the contribution of both bands as following,

$$\sigma = \sigma_e + \sigma_h, \quad (1S)$$

$$S = \frac{\sigma_e S_e + \sigma_h S_h}{\sigma_e + \sigma_h}, \quad (2S)$$

$$\kappa = \kappa_{lat} + \kappa_{carr} + \kappa_{bipolar}, \quad (3S)$$

$$\kappa_{carr} = L_e \sigma_e T + L_h \sigma_h T, \quad (4S)$$

$$\kappa_{bipolar} = \frac{\sigma_e \sigma_h}{\sigma_e + \sigma_h} (S_e - S_h)^2, \quad (5S)$$

where the subscript e and h represent the conduction band and valence band, respectively. Furthermore, the σ_i and S_i could be expressed by using Fermi–Dirac statistics,

$$\sigma_i = \sigma_{0,i} \frac{F_{1/2}(\xi_{f-i})}{\Gamma(3/2)}, i = e, h, \quad (6S)$$

$$S_i = \pm \frac{k_B}{e} \left(\frac{(s+5/2)F_{s+3/2}(\xi_{f-i})}{(s+3/2)F_{s+1/2}(\xi_{f-i})} - \xi_{f-i} \right), \quad (7S)$$

$$\delta_i = \frac{(s+5/2)F_{s+3/2}(\xi_{f-i})}{(s+3/2)F_{s+1/2}(\xi_{f-i})}. \quad (8S)$$

By introducing a new parameter $\gamma = \sigma_e / \sigma_h$ for simplification and the relationships of $\xi_{f-e} = \xi_f$ and $\xi_{f-h} = -\xi_f - \xi_g$, the definition of ZT, i.e., $ZT = S^2 \sigma T / \kappa$, could turns into following

$$ZT = \frac{\left(\delta_e - \xi_f - \frac{\delta_e + \delta_h + \xi_g}{1+1/\gamma} \right)^2 (1+\gamma)}{\left((B^*) \frac{F_{1/2}(\xi_f) / \Gamma(3/2)}{\xi_g} \right)^{-1} + \frac{(\delta_e + \delta_h + \xi_g)^2}{1+1/\gamma} + \left(\frac{e}{k_B} \right)^2 (L_e + \gamma L_h)}, \quad (9S)$$

$$B^* = \frac{1}{k_B} \left(\frac{e}{k_B} \right)^2 \frac{\sigma_{0,e}}{\kappa_{lat}} E_{g_joule}, \quad (10S)$$

Eq. (9S-10S) is just the exactly form we used in main text.

B. Calculation of m^* from Hall coefficient and Seebeck coefficient.

The carrier effective mass m^* was derived from the carrier density relationship with Fermi Dirac integral,

$$n = 2 \left(\frac{2\pi m^* k_B T}{h^2} \right)^{3/2} F_{1/2}(\xi_f), \quad (11S)$$

$$F_n(\xi_f) = \int_0^\infty \frac{\chi^n}{1 + e^{\chi - \xi_f}} d\chi \quad (12S)$$

Here, ξ_f was calculated from the measured Seebeck coefficient (S) with acoustic phonon scattering as dominant scattering mechanism, *i.e.*, $s = -1/2$.

$$S = \pm \left(\frac{(s + 5/2) F_{s+3/2}(\xi_f)}{(s + 3/2) F_{s+1/2}(\xi_f)} - \xi_f \right). \quad (13S)$$

The carrier concentration n was calculated from measured Hall coefficient (R_H) and Hall factor r_H ,

$$n = \frac{r_H}{e R_H}, \quad (14S)$$

$$r_H = \frac{3}{2} \frac{F_{1/2}(\xi_f) F_{-1/2}(\xi_f)}{(F_{-1/2}(\xi_f))^2}. \quad (15S)$$

C. Calculation of Lattice and bipolar thermal conductivity

Owing to the intrinsic excitation, the contribution of bipolar effect to the contribution of thermal conductivity needs to be taken into account to explain the widely observed raising tail of thermal conductivity at high temperature for most thermoelectric materials. The total thermal conductivity is composed of three parts as following,

$$\kappa_{tot} = \kappa_{lat} + \kappa_{carr} + \kappa_{bipolar} \quad , \quad (16S)$$

$$\kappa_{carr} = L\sigma T \quad , \quad (17S)$$

$$\kappa_{bipolar} = \frac{\sigma_e \sigma_h}{\sigma_e + \sigma_h} (S_e - S_h)^2 T \quad , \quad (18S)$$

where the κ_{tot} , κ_{lat} , κ_{carr} , and $\kappa_{bipolar}$ are the total, lattice, carrier, and bipolar thermal conductivity, respectively. The Lorenz number L is Fermi energy related parameter,

$$L = \left(\frac{k_B}{e} \right)^2 \left(\frac{(s+7/2)F_{s+5/2}(\xi_f)}{(s+3/2)F_{s+1/2}(\xi_f)} - \left(\frac{(s+5/2)F_{s+3/2}(\xi_f)}{(s+3/2)F_{s+1/2}(\xi_f)} \right)^2 \right) \quad , \quad (19S)$$

Here, the s is the scattering parameter based on the relaxation time approximation for the electronic transport. For acoustic phonon dominant scattering mechanism, s is $-1/2$. The reduced Fermi energy ξ_f near room temperature could be estimated from the Seebeck coefficient on the basis of single band approximation formula Eq. (13S). The reduced Fermi energy $\xi_f(T)$ at the higher temperature is required to solve the generalized charge neutrality equations (Eq. (20S-22S)) at a given temperature

$$n = p_0 + N_D \quad , \quad (20S)$$

$$n = 2 \left(\frac{2\pi m_e^* k_B T}{h^2} \right)^{3/2} F_{1/2}(\xi_f) \quad , \quad (21S)$$

$$p = 2 \left(\frac{2\pi m_h^* k_B T}{h^2} \right)^{3/2} F_{1/2}(-\xi_f - \xi_g) \quad , \quad (22S)$$

For the estimation of the $\kappa_{bipolar}$ according to Eq. (18S), we need estimated S_e , S_h , σ_e and σ_h . We can get S_e and S_h from Eq. (13S) by using the estimated $\xi_f(T)$, respectively. The estimation of σ_e and σ_h are based on the calculated carrier concentration and the fitting carrier mobility. m_e^* was obtained from the measured carrier concentration and Seebeck coefficient of $\text{Mg}_2\text{Sn}_{1-x-y}\text{Ge}_x\text{Sb}_y$ in this study, while $m_h^* = 1.3 m_0$ was used according to the Ref. [V. K. Zaitsev, CRC Press, New York, 2005]. μ_e was estimated from $(\sigma_e + \sigma_h)/(e(n+p))$, while u_h was used to fitting the temperature dependent σ and S . The temperature coefficient of the band gap of $\text{Mg}_2\text{Sn}_{1-x-y}\text{Ge}_x\text{Sb}_y$ were estimated from interpolation between the reported value for Mg_2Sn ($dE_g/dT = 3 \times 10^{-4} \text{eV/K}$) and Mg_2Ge ($dE_g/dT = 1.8 \times 10^{-4} \text{eV/K}$) from Ref. [V. K. Zaitsev, CRC Press, New York, 2005]. The effect of the dopant Sb and extra Mg on the dE_g/dT was neglected.

D. Calculation of band gap from the Fourier transform infrared spectrum

The Fourier transform infrared spectrums of selected samples were measured to derive the optical band gap. For near-normal incidence, the complex refractive index $n(\omega)$ and the extinction coefficient $k(\omega)$ with both the real and imaginary parts can be obtained from the Kramers-Kronig analysis as following,

$$n(\omega) = \frac{1 - R(\omega)}{1 + R(\omega) - 2[R(\omega)]^{1/2} \cos[\Theta(\omega)]}, \quad (23S)$$

$$k(\omega) = \frac{2[R(\omega)]^{1/2} \sin[\Theta(\omega)]}{1 + R(\omega) - 2[R(\omega)]^{1/2} \cos[\Theta(\omega)]}, \quad (24S)$$

where $\Theta(\omega)$ is the phase shift, which is,

$$\Theta(\omega) = \frac{\omega}{\pi} \int_0^\infty \frac{\ln[R(\omega')] - \ln[R(\omega)]}{\omega^2 - \omega'^2} d\omega'. \quad (25S)$$

The extinction coefficient $k(\omega)$ is used to calculate the frequency dependent absorption coefficient $\alpha(\omega)$ through the relation,

$$\alpha(\omega) = 4\pi\omega k(\omega). \quad (26S)$$

Finally, the $(\alpha h\nu)^{1/2}$ was plotted as a function of the energy $h\nu$, as shown in Fig. S7. The across point of the dash line with $h\nu$ axis was used to determine the band gap

E. Connections among the components of B^*

It is worthy pointing out that the components (U^* , E_g , and κ_{lat}) determining the material parameter B^* are still interconnected with each other from a more fundamental point of view. Here, we show a simple discussion about the deeper relation between U^* and E_g . Firstly, Let us to recall the defination of U^* in the main body ,

$$U^* = \mu (m^*/m_0)^{3/2} T^{3/2} \quad (S27)$$

Then, we replace the carrier effective mass term $(m^*)^{3/2}$ in the defination of U^* with $N_v(m_b^*)^{3/2}$ where m_b^* and N_v are the band effective mass m_b^* and the number of degenerate band valley N_v , respectively.

$$U^* = \mu N_v (m_b^*/m_0)^{3/2} T^{3/2} \quad (S28)$$

Considering the acoustic phonon as dominant carrier scattering mechanism for most thermoelectric materials, μ in Eq. (S28) could be further evolved using the deformation potential E_d , elastic constant C_l (Similar treatment could be found in Ref. 9.), and then Eq. (S27) turns into,

$$U^* \propto \frac{N_v C_l}{(m_b^*/m_0) E_d} \quad (S29)$$

According to Eq. S29, a larger N_v and smaller m_b^* are favorable for higher U^* . Now the material parameter B^* could be rewritten as,

$$B^* \propto \frac{N_v C_f}{E_d \kappa_{lat}} \frac{E_g}{(m_b^*/m_0)} \quad (\text{S30})$$

Based on the k-p perturbation theory, m_b^* is related to E_g , conduction band wave function Γ_c , and valance band wave function Γ_v .

$$\frac{1}{m_b^*} = \frac{1}{m_0} + \frac{2|\langle \Gamma_c | k \cdot p | \Gamma_v \rangle|^2}{m_0^2 k^2 E_g} \quad (\text{S31})$$

This relation essentially describes the fact that the effective mass of a free electron in one band changes due to the coupling to the electrons in other bands. For non-degenerate conduction band electrons, it has been shown that a material with larger E_g usually has a heavier m_b^* that corresponds to a lower mobility, according to Ref. 55. According to the data for typical V (Ge), III-V (GaN, GaAs, GaSb, InP, InP and InAs), II-VI (ZnS, SnSe, ZnTe, CdTe) semiconductor, the ratio of $E_g/(m_b^*/m_0)$ decreases with increase of band gap. This simplified picture partly explains why most of the well-known thermoelectric materials are narrow band semiconductor. However we want to caution that for thermoelectric materials where heavy atoms are usually involved, spin-orbit coupling needs to be considered and the above formalism needs to be carefully examined with more details. Additionally, the controllable doping for many semiconductors with wide band-gap are still a technical challenge which also prevents people from more widely investigating their thermoelectric performance. Further explorations into the relation among the parameters in generalized material parameter B^* , described in Eq. S28, would be more insightful to guide the researcher to atomically construct ideal materials with optimized atomic sizes, bonding strengths, and crystalline structures.

F. Estimated U^* from measured S and σ

For the samples without data from Hall measurement in the Table S1, including CoSbTe, CoSbTeSn, ingot-BiSbTe, nano-BiSbTe, and PbTe-1, U^* s were estimated from the measured Seebeck coefficient S and electrical conductivity σ at room temperature as following,

$$S = \pm \frac{\kappa_B}{e} \left(\left(s + \frac{5}{2} \right) - \xi_f \right) \quad (\text{S32})$$

$$\sigma = 2e \left(\frac{2\pi m_0 k_B T}{h^2} \right)^{3/2} (m^*/m_0)^{3/2} \mu \exp(\xi_f) = A \cdot U^* \exp(\xi_f) \quad (\text{S33})$$

Here, A is a constant for simplification,

$$S = \pm \frac{\kappa_B}{e} \left(\left(s + \frac{5}{2} \right) + \ln A + \ln U^* - \ln \sigma \right) \quad (\text{S34})$$

$$U^* = \exp \left\{ \left(\left| S \right| \frac{e}{\kappa_B} \right) + \ln \sigma - \left(s + \frac{5}{2} \right) + \ln A \right\} \quad (\text{S35})$$

The error bar for U^* by using this method should be similar to that of the term $\mu (m^*/m_0)^{3/2}$, which has been discussed in *Chem. Mater.* 2008, **20**, 7526-7531.